Dynamic Interactions Between the Southern San Andreas Fault and Normal Faults in the Brawley Seismic Zone

[1]Luis I. Bazán, [1]Christodoulos Kyriakopoulos, [2]David Oglesby, [3]Aron Meltzner, [4]Thomas Rockwell and [5]John Fletcher;
[1]CERI, University of Memphis; [2]UC Riverside ; [3]Earth Observatory of Singapore (NTU); [4]San Diego State University; [5]CICESE.

Contact info: lbznflrs@memphis.edu

1. Introduction and Background

We investigate the initiation phase and subsequent triggering of the Southern San Andreas Faut (SSAF) by adjacent smaller faults that could serve as nucleation points and/or participate in larger multi-fault ruptures. Our target area of investigation is the Brawley Seismic Zone (BSZ), which is characterized by intense micro-seismicity and seismic swarm sequences. The seismic activity mainly occurs along vertical left-lateral strike-slip cross faults that intersect the SSAF at several locations south of Bombay Beach, CA. However, there is also evidence that displacement in the northern BSZ occurs along normal faults (Brothers et al., 2009, Brothers et al., 2011) under the Salton Sea, which could also interact with the SSAF. For these reasons, both the cross-faults and the normal faults in this area should be considered as potential initiation structures as well as faults participating in future multi-fault earthquakes. Here we extend our previous work regarding the dynamic interactions between the SSAF, the Imperial Fault (IF), and the system of cross faults (Kyriakopoulos et al., 2019) to include the possible interaction between the SSAF and a normal fault under the Salton Sea. To achieve our goal, we generated a series of dynamic rupture scenarios that help us illuminate the following: a) the mechanisms by which SSAF events can transfer slip onto the normal faults; and b) how normal fault earthquakes could trigger a major event on the SSAF.

To explore the dynamic interactions between the SSAF and the Normal Fault, we run models using the dynamic rupture code FaultMod (Barall, 2009; see table 1 in box 2 for computational parameters). The mesh required to run the dynamic simulations is presented in box 3.

2. Simulation of Earthquakes

We assume a homogenous and isotropic medium. The friction law is slip weakening, where the friction coefficient drops from a static value of 0.6 to a dynamic value of 0.1 over a slip weakening distance of 0.3 m (see figure to the right). We calibrate the initial stress conditions in our models by using the seismic parameter S,

$$S = \frac{\mu_{static} * \sigma_0 - \tau_0}{\tau_0 - \mu_{sliding} * \sigma_0} \quad \begin{matrix}\text{(Strength Excess)}\\ \text{(Stress Drop)}\end{matrix} \quad \text{Andrews et al., 1976}$$

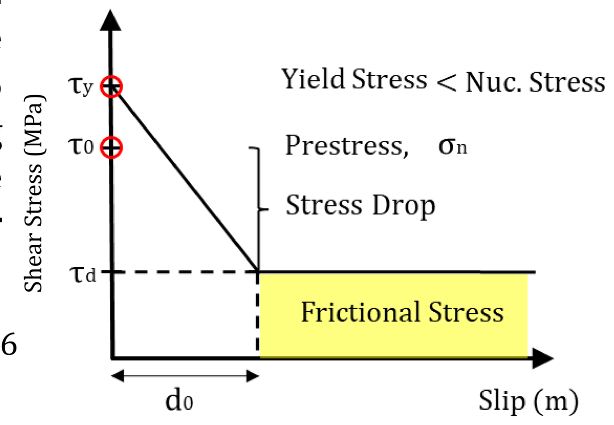

Small values of S indicate a system closer to failure while high S values indicate the opposite. In our models we test two prestress conditions, S=0.45 and S=2.0, combined with two fault geometric configurations and three nucleation locations (see Figure below). The first configuration assumes that the SSAF stops at Bombay Beach while the second one includes an extension of the SSAF south of Bombay Beach. Our postulated extended SSAF is based on the interpretation of seismicity and faults in the Brawley Seismic Zone presented in Kyriakopoulos et al., 2019.

τ_0 initial shear stress (MPa)	4.33, 2.6
σ_0 initial normal stress (MPa)	9.76
τ_0 Nucleation stress (MPa)	6.44
Static friction (μ_s)	0.6
Dynamic friction (μ_d)	0.1
Slip weakening distance (m)	0.3
Density (Kg/m^3)	2700
S-wave speed (m/sec)	3162
P-wave speed (m/sec)	5477
Nucleation radius (m)	5000
Nucleation speed (m/sec)	2000
Fault element Size (m)	~150
Off-fault element size (m)	~450
Rupture time step (sec)	10^2

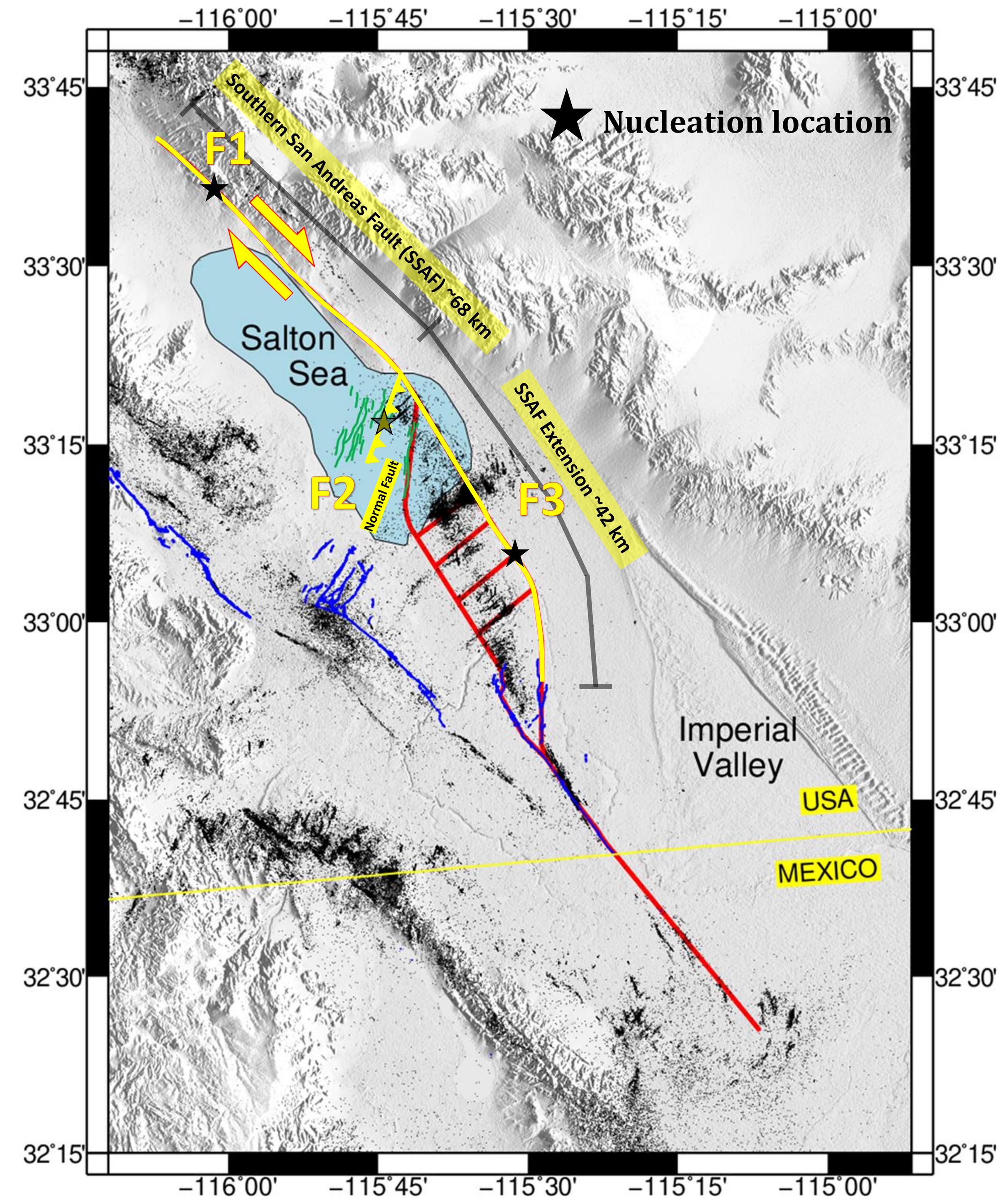

3. Finite Element Model

The finite element mesh required to run the dynamic rupture simulations is generated using TRELIS 17.1 (Coreform.com). The size of the FEM total domain is ~120 x 120 km and is composed by over 17 million hexahedral elements. The size of the elements in the volumes hosting the faults is ~150 m and increases to ~450 m or larger outside the high-density area. In our models we test two configurations for the Southern San Andreas Fault: 1) The fault ends at Bombay beach (length ~68 km), and 2) The fault continues south of Bombay Beach and under the Salton Sea and stops near Brawley city (length ~112 km). The Normal Fault (NF) is 15 km long and dipping SE at 65°. In all our simulations the locking depth is 15 km.

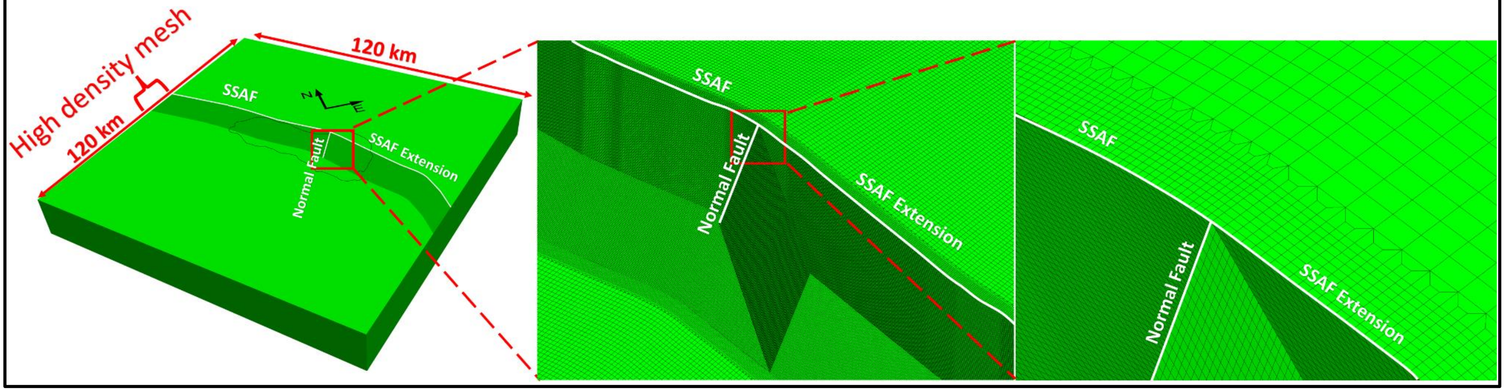

4. Final Fault Slip: Nucleation on the SSAF

Configuration 1: SSAF ends at Bombay Beach
Nucleation north of the Normal Fault

★ Nucleation location

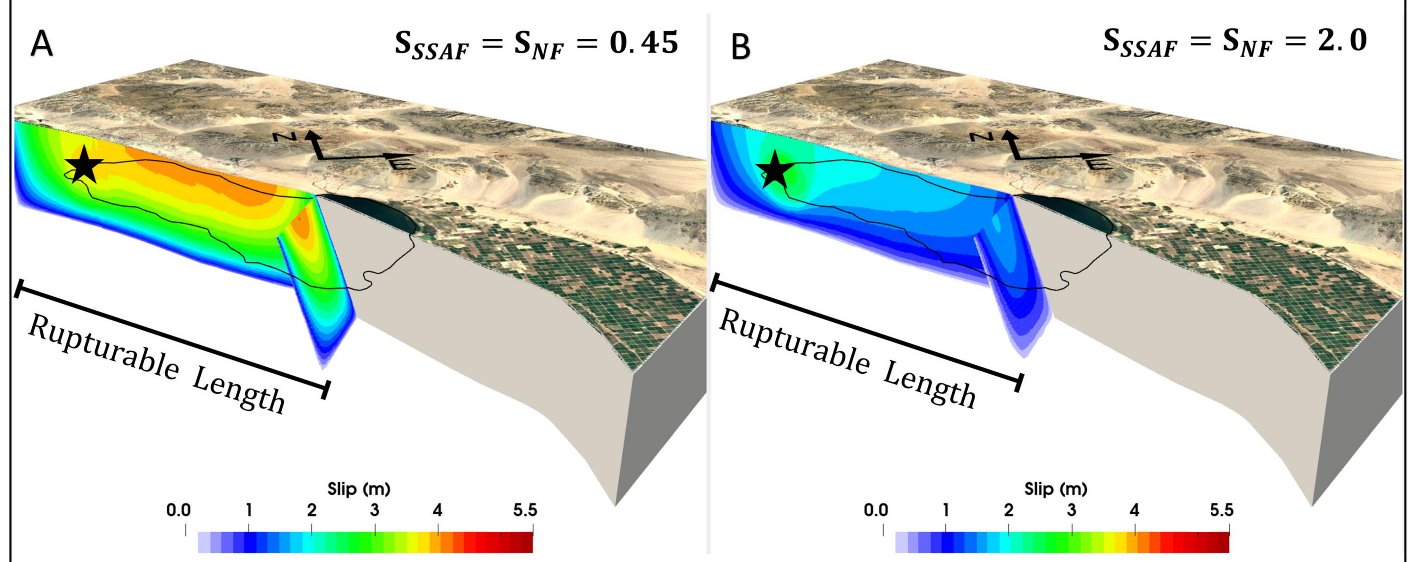

Configuration 2: SSAF extends south of Bombay Beach
Nucleation north of the Normal Fault

★ Nucleation location

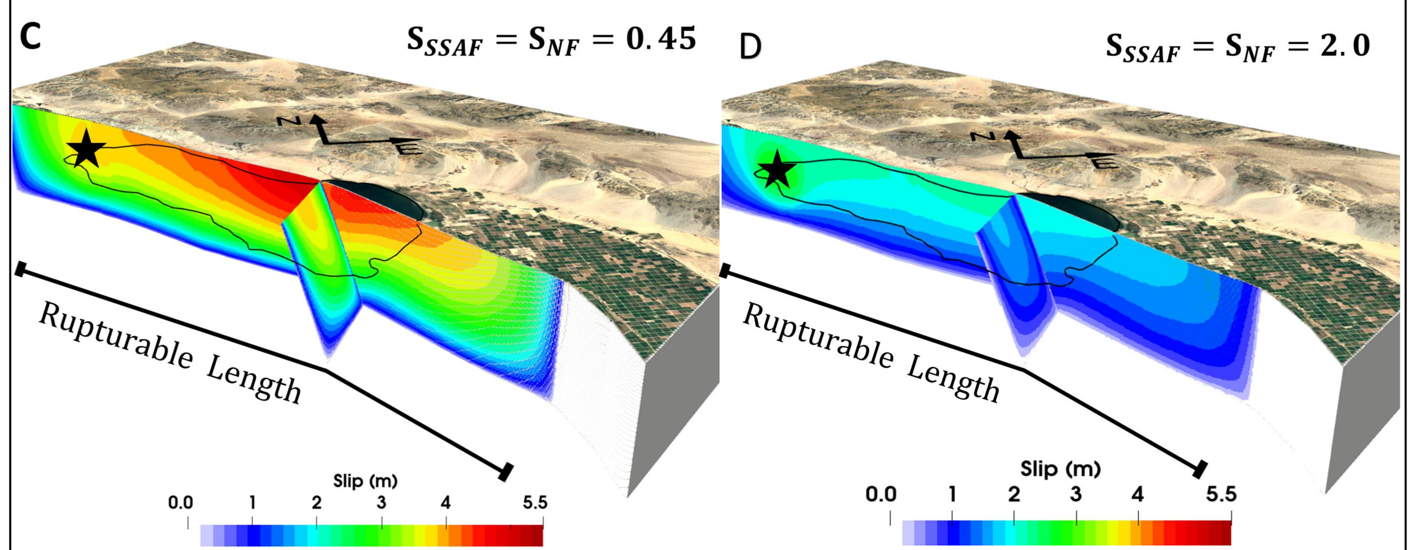

Configuration 2: SSAF extends south of Bombay Beach
Nucleation south of the Normal Fault

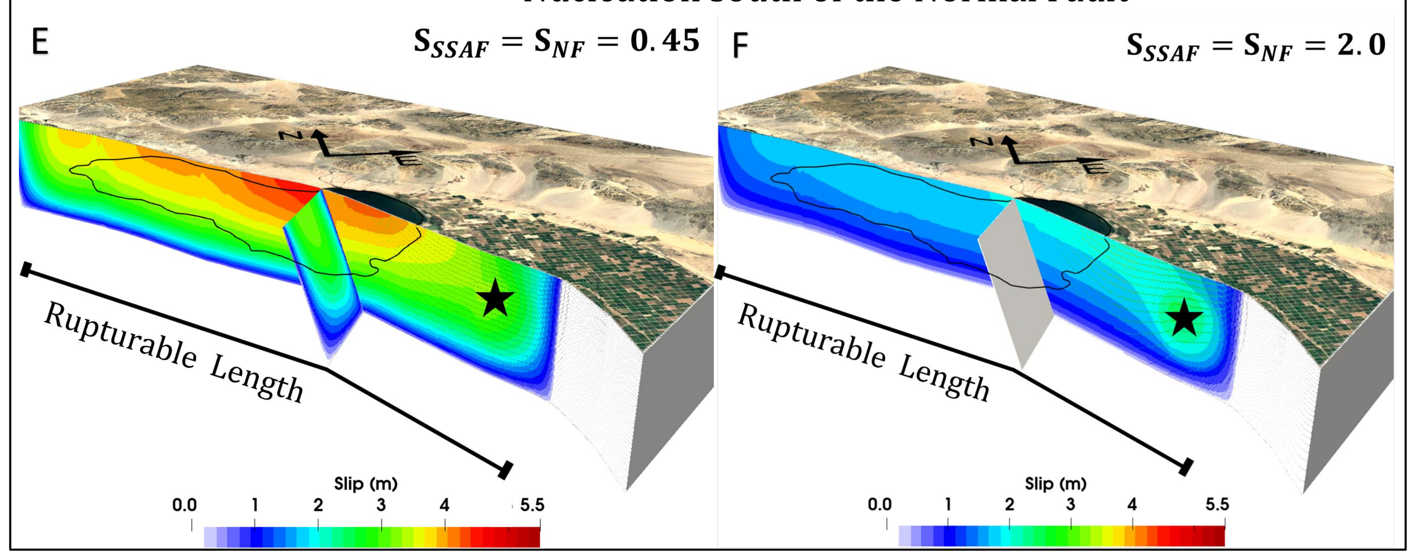

5. Final Fault Slip: Nucleation on Normal Fault

Configuration 1: SSAF ends at Bombay Beach

★ Nucleation location

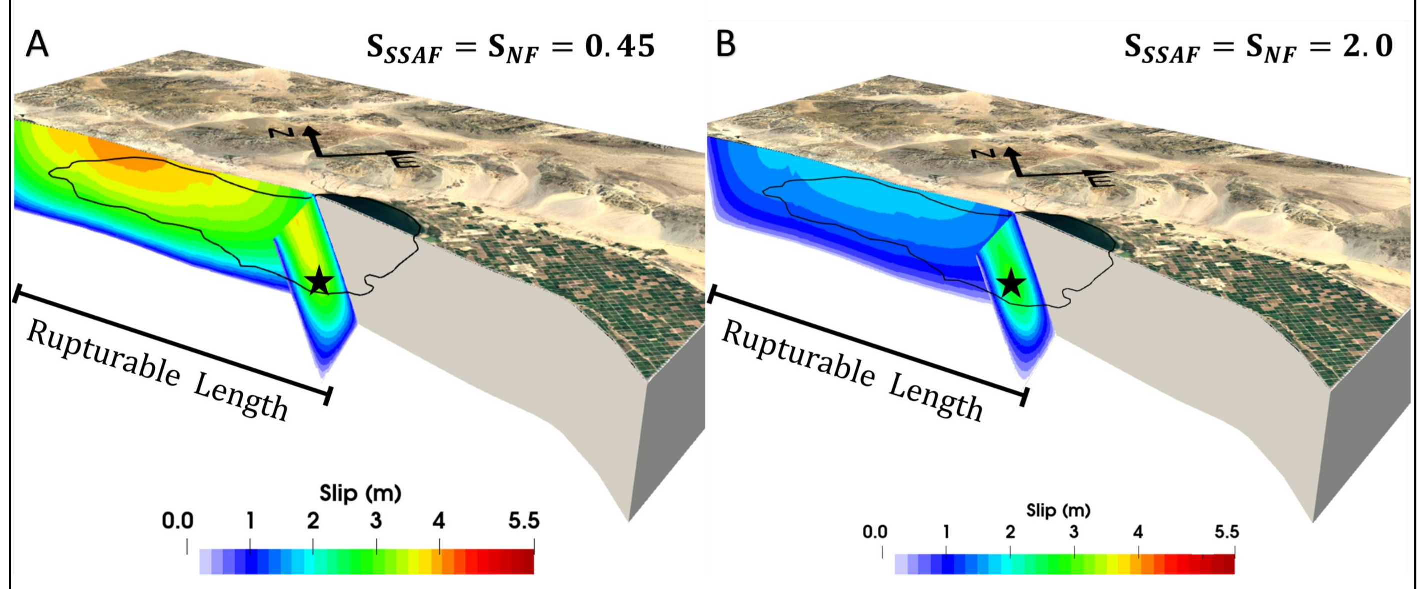

Configuration 2: SSAF extends south of Bombay Beach

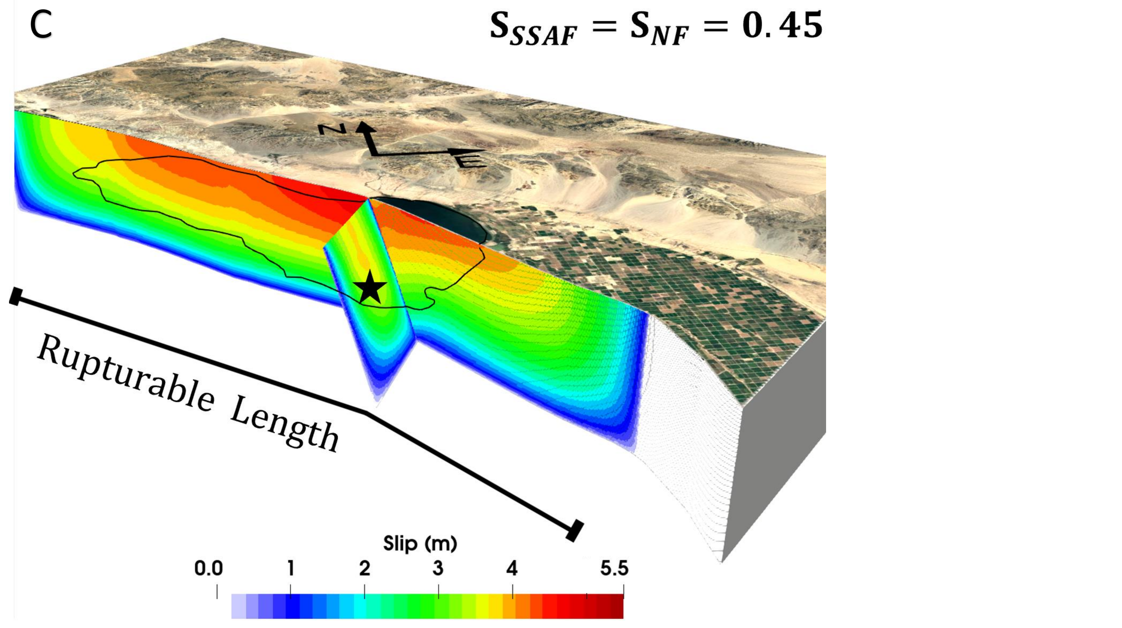

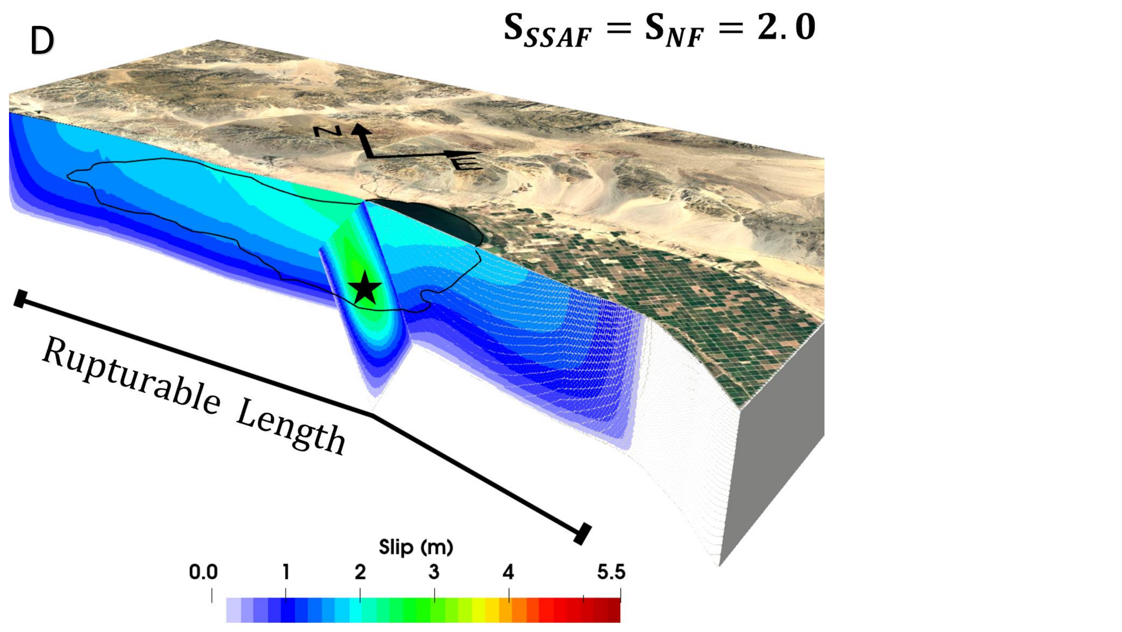

6. Preliminary Results and Conclusions

Our preliminary results indicate that the nucleation location plays a determining role in the triggering of slip on the SSAF or the Normal Fault. Based on our current assumptions regarding fault geometry and prestress conditions, we find that:

- Simulations with nucleation on the SSAF north of the Normal Fault (north to south propagation) are able to trigger slip on the Normal Fault.
- Simulations with nucleation on the SSAF south of the Normal Fault (south to north propagation) produce initially unfavorable conditions for rupture on the Normal Fault. When the rupture passes the SSAF-NF intersection, this effect is reversed.
- Earthquakes with nucleation on the Normal Fault propagate into the SSAF.

The results described here depend on the competing effects of time dependent normal and shear stresses changes. Ruptures approaching the SSAF-NF intersection from the north generate a dynamic decrease of normal stress and increase of shear stress on the normal fault, favoring rupture to the normal fault. In contrast, ruptures approaching from the south produce the opposite effect. In the coming year we are planning to extend our investigation with models using prestress conditions based on the regional stress tensor, and possible variations of the normal fault geometry.

References

- Andrews, D. J. (1976). Rupture velocity of plane strain shear cracks. Journal of Geophysical Research, 81(32), 5679-5687. https://doi.org/10.1029/JB081i032p05679
- Barall, M. (2009). A grid-doubling finite-element technique for calculating dynamic three-dimensional spontaneous rupture on an earthquake fault. Geophysical Journal International, 178, 845–859; doi:10.1111/j.1365-246X.2009.04190.x
- Brothers, D. S., Driscoll, N. W., Kent, G. M., Harding, A. J., Babcock, J. M., & Baskin, R. L. (2009). Tectonic evolution of the Salton Sea inferred from seismic reflection data. Nature Geoscience, 2(8), 581-584. https://doi.org/10.1038/ngeo590
- Kyriakopoulos, C., Oglesby, D. D., Rockwell, T. K., Meltzner, A. J., Barall, M., Fletcher, J. M., & Tulanowski, D. (2019). Dynamic rupture scenarios in the Brawley Seismic Zone, Salton Trough, southern California. Journal of Geophysical Research: Solid Earth, 124, 3680-3707. https://doi.org/10.1029/2018JB016795